



Chromospheric evaporation seen in hard X-rays

Z. J. Ning *

Key Laboratory of Dark Matter and Space Astronomy, Nanjing 210008, China
Purple Mountain Observatory, Nanjing 210008, China

Abstract. Chromospheric evaporation implies the mass flow from chromosphere to corona along the loop legs in the solar flares, indicating the targets of hard X-ray emissions movement in the flare loops. From observations, hard X-rays tend to rise up the double footpoint sources along the loop legs and finally merge together around the top at the same position as the loop top source. After Reuven Ramaty High Energy Solar Spectroscopic Imager (RHESSI), the evidence of chromospheric evaporation in hard X-rays are studied and analyzed in several events. The source motions caused by the chromospheric evaporation are not observed at the whole energy band of hard X-rays, but favorably seen at 10-30 keV. Hard X-ray sources at the high energy (i.e. above 50 keV) would never show motions and stay around the footpoint during the evaporation. The observational results show that the typical velocity of hard X-ray source motions ranges from 200 km s^{-1} to 500 km s^{-1} , the typical timescale of source merger is around 60 s (between 30 and 80 s).

Keywords : Sun: flares – Sun: X-rays – Sun: chromosphere

1. Introduction

From the standard flare model, the magnetic reconnection is believed to be the primary energy release mechanism to heat the plasma and accelerate electrons high in the corona. These electrons travel downward to the chromosphere and transfer their energy into the thermal energy to heat the local material rapidly through the collisions with the chromospheric plasma. The resulting overpressure drives a mass flow upward along the legs, thus filling the loop or its constituent strands during the flare impulsive phase. This process is well known as the “chromospheric evaporation” in solar flares

*email: ningzongjun@pmo.ac.cn

(e.g. Fisher, Canfield & McClymont, 1985a,b,c; Liu et al. 2004; 2006; Ning et al. 2009). Observational evidence of chromospheric evaporation has been documented in X-ray (e.g. Liu et al., 2006; 2008; Ning et al., 2009; Ning & Cao, 2010), EUV (i.e. Fludra et al., 1989; Mariska, 1994; Milligan et al., 2006a; 2006b; Milligan & Dennis 2009; Brosius, 2001; 2003; 2009), and radio emission (Aschwanden & Benz, 1995; Karlicky, 1998; Ning et al. 2009).

2. Observations

With its full disk solar imaging capability, wide energy coverage (3-17,000 keV), and high sensitivity, RHESSI (Lin et al. 2002) provides unprecedented capabilities for investigating the X-ray source motions at different energy bands with a high temporal resolution after the chromospheric evaporation. In this paper, we present the hard X-ray evidences of chromosphere evaporation detected in three solar flares.

Fig. 1 shows the evolution of the 2004 October 30 flare images in six different energy bands, i.e. 6-9 keV, 9-12 keV, 12-15 keV, 15-20 keV, 20-30 keV, 30-50 keV. The front segments of detectors 3-8 excluding 7 are used for reconstructing these RHESSI images with a 20 s integration window. Before 03:30:00 UT which corresponds to the maximum of the light curve at 25-15 keV, the X-ray emission mainly comes from the flare loop at lower energies from 6-15 keV. The hard X-ray footpoints appear at a wide energy range from 12-50 keV at 03:30:00 UT, although the emission from the loop top source also extends toward the legs at the low energy of 6-12 keV. Subsequently, the two footpoints tend to move close to each other, and the projection distance between them gradually decreases, finally merging into a single source. This process is more clearly seen from the evolution of the 20-30 keV images. At 03:29:40 UT, the flare shows double footpoint sources, which moved closer after 20 s, and 20 s later, they closed even more than before. And at 03:30:40 UT, they became an elongated source. Then the length of the source decreased, and finally showed a curved shape at 03:31:40 UT. The source was located at the same position as the thermal loop top source. The merging timescale is dependent on energy. The higher energy X-rays show a longer timescale, as the dashed line in Fig. 1 indicates. This shows that the hard X-ray emissions are the result of continually accelerated electrons impinging upon the increasingly dense loop, and that higher energy X-rays originate from the deeper layers of the flaring legs. Until 03:31:40 UT, this flare exhibits a single source at all energy bands from 6-50 keV. This is expected as a common feature of the flare due to chromospheric evaporation, which increases the plasma density in the loop, making the loop top source dominant at progressively higher energies.

Fig. 2 shows the spatial evolution of the RHESSI CLEAN images at 10-15 keV for the 2004 December 1 flare. This flare displays two footpoint sources at the hard X-rays, especially at 10-15 keV, while a looptop source at the soft X-rays of 6-10 keV at 07:04:20 UT. Left-top shows the MDI magnetic field with the RHESSI X-ray contours at 6-10 keV and 10-15 keV. The south footpoint source (10-15 keV) is in the negative

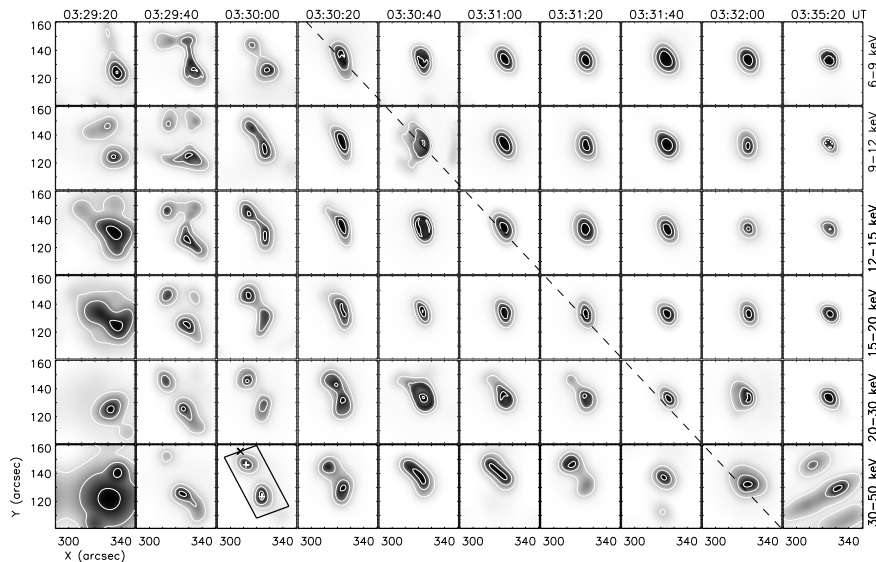


Figure 1. RHESSI PIXON images at different energies (rows) and different times (columns) for the 2004 October 30 solar flare. Contour levels are set at 20%, 50% and 90% of the maximum brightness of each image. The parallelogram is considered as the loop projection on the disk. The footpoint sources at 30-50 keV are marked by two pluses.

polarity field area, while the north source does not overlap with the strongest positive polarity at all (possibly due to the projection effect). The looptop source is located between them. Such morphology displays the typical characteristics of solar flare in the X-ray observations. And it is consistent with the standard flare model. The looptop source is close to the north footpoint. Then, both footpoint sources shift their positions at 07:04:20 UT, and move towards each other afterwards. Finally, they merge into a single hard X-ray source at 07:05:20 UT. As shown in Fig. 2, the merger takes about 60 s, between 07:04:20–07:05:20 UT. However, the looptop source of 6-10 keV keeps the same position during this interval. In order to describe the merger motion of the hard X-ray sources, we measure the linear distance between the two footpoints at 10-15 keV. As given in Fig. 2, the distance (L) is about 34.2 arcsec at 07:04:20 UT, then L is shortened to about 15.8 arcsec at 07:05:00 UT. At 07:05:20 UT, the two sources become one single source. The measured merger speed is about 428 km s^{-1} . Note that we do not consider the projection effect here. The previous observations show that the different energies of the X-rays could be of different origin. The radiation of the energy 10-15 keV may be considered as thermal emission from the evaporated plasma or as non-thermal emission from the precipitating electrons, or, probably a mixture of both kinds of the radiation. Subsequently, the flare just shows a single source, as shown in Fig. 2 (right-bottom), in the looptop with a broad energy band from 6-15 keV until 07:07:40 UT.

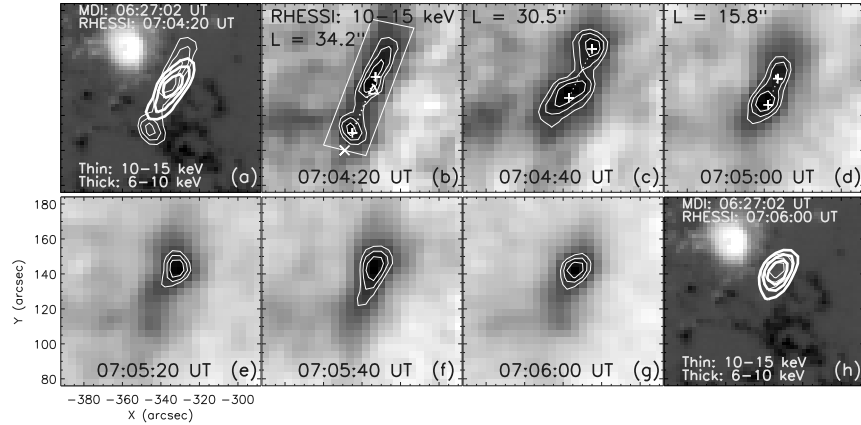


Figure 2. MDI map of magnetic field at 06:27:02 UT, showing the sunspots with positive (white) and negative (black) polarities with RHESSI X-ray contours at 07:04:20 UT (a), or at 07:06:00 UT (h), and RHESSI CLEAN 10-15 keV images (b, c, d, e, f, g) at six different times for the 2004 December 12 solar flare. All contour levels are set at 70%, 80%, and 90% of the maximum brightness for 10-15 keV (thin lines) or 6-10 keV (thick lines) images. The plus symbols represent the positions of maximum brightness at both footpoints, and the values of L measure the distance (dashed lines) between them.

Figure 3 shows the GOES and RHESSI observations of the 2003 November 13 solar flare. The gray patch marks the time interval over which the X-ray source movements have been studied in detail. Bottom panel shows the time evolution of the 20-22 keV brightness distribution along the flare loop from one footpoint of FP_1 to another (FP_2). The looptop source could be located at the middle of the loop, while the double footpoints are at two ends. The local maximum of the brightness are traced by two lines (marked by asterisks and pluses) corresponding to the location changes of FP_1 and FP_2 . At the flare beginning, there are two subpeaks of brightness along the loop, while only one brightness peak in the later phase. The solid lines present the linear fitting and their velocities are given. This flare shows double source at the beginning, and then tends to move close and merges around 04:59 UT. However, after 05:00 UT, this event displays double footpoint sources again.

3. Summary

We present the hard X-ray evidences of chromospheric evaporation in three examples of solar flares observed by RHESSI. As that is expected from the standard flare model, the hard X-ray targets would display motions after the chromospheric evaporation. Observationally, the flare shows the double footpoint movement along the loop legs upward. Such kinds of source motions are only seen at the middle energy band, i.e., 10-30 keV. The flare does not move the footpoint sources at the high energy (i.e., above 50 keV). The typical timescale of the motion is dependent on the energy,

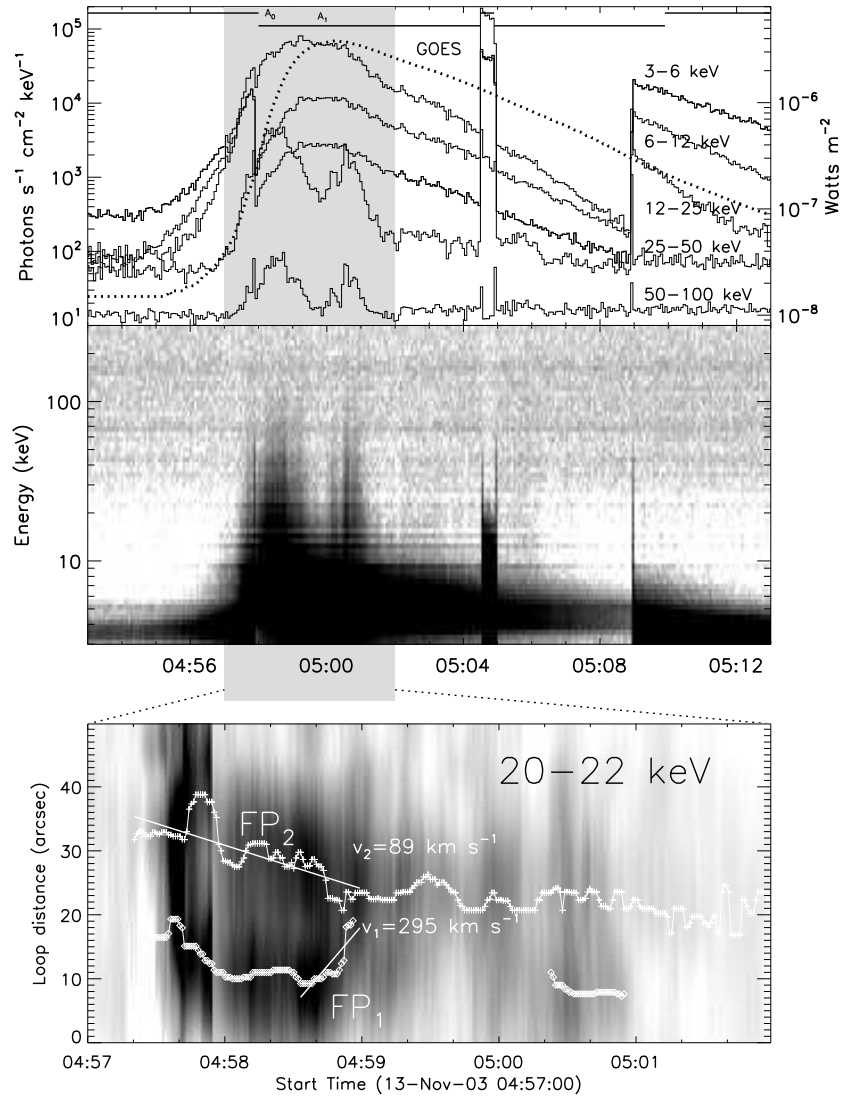


Figure 3. Top: RHESSI (solid) and GOES 1-8 Å (dot) light curves for the 2003 November 13 solar flare. RHESSI energy bands are 3-6 keV, 6-12 keV, 12-25 keV, 25-50 keV, and 50-100 keV, with corresponding scaling factors 1, 1/2, 1/2, 1/5, and 1/10 respectively. RHESSI attenuators are shown with the thick line on the top. Middle: RHESSI 3-300 keV X-ray emissions as a function of time, and the intensity jumps are due to RHESSI attenuator effects. Bottom: time evolution of 20-22 keV brightness along the flare loop from the FP₁ to FP₂ during the interval with gray in top panel. Plus symbols correspond to FP₂ and the asterisks correspond to FP₁. White solid lines represent the linear fitting of the associated points.

between 30 and 80 s, and movement speed is several hundreds km s^{-1} . This kind of X-ray source motion is different from another one, which is observed as the separation movement with three sub-types from both YOHKOH and RHESSI observations -- perpendicular (Type I), parallel (Type II) or anti-parallel (Type III) to the magnetic neutral line (Bogachev et al. 2005; Gan, Li & Miroshnichenkov, 2008; Yang et al. 2009; Liu et al. 2010). It must be understood that this kind of motion is not a material motion, but shows the changing location of lower-atmosphere excitation. From hard X-ray observations, this kind of motions are independent on the energy. In other words, hard X-ray sources display the same motions on the whole energy band.

Acknowledgements

This work is supported by NSF of China under grants 10833007, 40804034, 10973042, 973 Program under grant 2011CB811402 and Laboratory No. 2010DP173032.

References

- Aschwanden M. J., Benz A. O., 1995, *ApJ*, 438, 997
Bogachev S.A., Somov B.V., Kosugi T., Sakao T., 2005, *ApJ*, 630, 561
Brosius J.W., 2001, *ApJ*, 555, 435
Brosius J.W., 2003, *ApJ*, 586, 1417
Brosius J.W., 2009, *ApJ*, 701, 1209
Fludra A., Bentley R.D., Lemen J.R., Jakimiec J., Sylwester J., 1989, *ApJ*, 344, 991
Fisher G. H., Canfield R. C., McClymont A. N., 1985a, *ApJ*, 289, 414
Fisher G. H., Canfield R. C., McClymont A. N., 1985b, *ApJ*, 289, 434
Fisher G. H., Canfield R. C., McClymont A. N., 1985c, *ApJ*, 289, 425
Gan W.Q., Li Y.P., Miroshnichenko L.I., 2008, *AdSpR*, 41, 908
Karlicky M. 1998, *A&A*, 338, 1084
Lin R.P. et al., 2002, *Solar Phys.*, 210, 3
Liu W., Jiang Y.W., Liu S., Petrosian V., 2004, *ApJL*, 611, 53
Liu W., Liu S., Jiang Y.W., Petrosian V., 2006, *ApJ*, 649, 1124
Liu W., Petrosian V., Dennis B.R., Jiang Y.W., 2008, *ApJ*, 676, 704
Liu C., Lee J., Jing J., Liu R., Deng N., Wang H., 2010, *ApJL*, 721, 193
Mariska J.T., 1994, *ApJ*, 434, 756
Milligan R.O., Gallagher P.T., Mathioudakis M., Keenan F.P., 2006a, *ApJL*, 642, 169
Milligan R.O., Gallagher P.T., Mathioudakis M., Bloomfield D.S., Keenan F.P., Schwartz R.A., 2006b, *ApJL*, 638, 117
Milligan R.O., Dennis B.R., 2009, *ApJ*, 699, 968
Ning Z., Cao W., Huang J., Huang G., Yan Y., Feng H., 2009, *ApJ*, 699, 15
Ning Z., Cao W., 2010, *ApJ*, 717, 1232
Yang Y.-H., Cheng C.Z., Krucker S., Lin R.P., Ip W.H., 2009, *ApJ*, 693, 132